MAUSAM, **76**, 4 (October 2025), 1095-1112

MAUSAM

DOI: https://doi.org/10.54302/mausam.v76i4.7086
Homepage: https://mausamjournal.imd.gov.in/index.php/MAUSAM

UDC No.502.13:551.588.6(540.27)

From flames to recovery: ecosystem resilience in Uttarakhand's 2022 forest fires

M.S. SHYAM SUNDER[1#], SHANTI SHWARUP MAHTO[2] and BHISHMA TYAGI[1*],

[1]*Department of Earth and Atmospheric Sciences, National Institute of Technology Rourkela, Rourkela 769008, India. (#521er1012@nitrkl.ac.in)*

[2] *Department of Geoinformatics, Central University of Jharkhand, Ranchi – 835222, India. (ssmahto.dgi@cuj.ac.in)*

(*Received 10 October 2024, Accepted 15 April 2025*)

***Corresponding author's email: tyagib@nitrkl.ac.in**

सार – हिमालय की तलहटी भारत में जंगल की आग के प्रमुख केंद्रों में से एक है। गर्म-शुष्क ग्रीष्म ऋतु (मार्च-जून) के दौरान जंगल की आग अक्सर वन पारिस्थितिकी तंत्र को नुकसान पहुंचाती है, ऐसी ही एक घटना 2022 में उत्तराखंड की आग है, जिसने प्राकृतिक वनस्पति को गंभीर रूप से प्रभावित किया और आर्थिक नुकसान हुआ। हालाँकि, इसके चालकों और वनस्पति प्रभावों के लिए पारिस्थितिकी तंत्र के लचीलेपन को अच्छी तरह से समझा नहीं गया है। हाइड्रोक्लाइमैटिक, वनस्पति और आग के डेटासेट का उपयोग करते हुए, हमने स्थानिक-कालिक विविधताओं और जली हुई वनस्पति की वसूली की पूरी तरह से जांच की। उच्च-गंभीरता वाले जले हुए उत्तराखंड के दक्षिणी क्षेत्रों में केंद्रित थे, जिनकी व्याख्या dNBR सूचकांक वर्गों के आधार पर की गई थी। चयनित उच्च गंभीरता वाले क्षेत्र के लिए गणना किए गए जले हुए बायोमास में गिरावट (16.75%) दिखाई दी उपग्रह प्रेक्षण सूचकांकों ने आग की घटना के तुरंत बाद गतिशील बहाली देखी, SAVI (~0.23 - 0.43) और VCI (~40 - 80) दिखाया, जो द्वितीयक अनुक्रमण का संकेत देता है। कुल मिलाकर, आग लगने के बाद जले हुए क्षेत्रों में SH>40% और LH<−20% था, लेकिन GPP (~20%) और ET (8-21%) में गिरावट देखी गई, जबकि PET में वृद्धि हुई, जिससे कमजोर सतही आपूर्ति (3-19%) के तहत वायुमंडलीय माँग में वृद्धि हुई, जिसने धीमी गति से सुधार की व्याख्या की। यह अध्ययन वनस्पति गतिशीलता के आकलन और समझ के महत्व पर प्रकाश डालता है, साथ ही वायुमंडलीय स्थितियों और वनस्पति सुधार की आंतरिक विशेषताओं के बारे में महत्वपूर्ण जानकारी प्रदान करता है, जो वन अग्नि प्रभावों के अनुकूल होने के लिए मार्गदर्शन प्रदान करता है।

ABSTRACT. The foothills of the Himalaya are one of the major hotspots of forest fires in India. Forest fires during the hot-dry summer season (March-June) often cause damage to the Forest ecosystem, one of such events is the Uttarakhand fires in 2022, which seriously impacted the natural vegetation led to economic losses. However, its drivers and ecosystem resilience to vegetation impacts are not well understood. Using hydroclimatic, vegetation, and fire datasets, we thoroughly examined the spatio-temporal variations and recovery of burnt vegetation. High-severity burns were concentrated in the southern regions of Uttarakhand, interpreted based on the dNBR index classes. The burned biomass calculated for the selected high severity area, showed decline (16.75%), post-fire recovery (40.85%) indicated uneven ecosystem resilience. High VPD and low soil moisture, intensified the fire risks but during monsoon onset and fire-induced rainfall helped restore soil moisture and reduce VPD, supported early vegetation recovery. The satellite observation indices observed dynamic restoration immediate after the fire event, showed SAVI (from ~0.23 – 0.43) and VCI (from ~40 - 80), indicating secondary succession. Overall post-fire burned regions had SH>40% and LH<−20% but showed decline in GPP (~20%) and ET (8-21%), while PET rose stronger atmospheric demand under weakened surface supply (3-19%), which the explained slow recovery. This study highlights the importance of assessing and understanding the vegetation dynamics with providing key insights into atmospheric conditions and internal characteristics of vegetation recovery offers guidance for adapting to forest fire impacts.

Key words – Vegetation dynamics, Secondary succession, Biomass and microbial interaction, Post-fire recovery.

1. Introduction

Forest fires, with their inherently disruptive nature, pose a significant threat to both ecological balance and socio-economic systems, demanding for urgent and comprehensive scientific investigation. Forest fires are natural processes associated with intense heat, dryness, and vegetation dynamics (Sahu *et al.,* 2022). The frequency, intensity, and impacts of forest fire have been exacerbated by anthropogenic activities and climate change in the recent decades (Jones *et al.,* 2022). As per the report of the Global Forest Resource Assessment, the global degradation of forest covers and the unusual conversion of land covers with poor management are the most supporting factors for forest fires, globally. For instance, in 2015 alone, forest fires have damaged over 98 million hectares of forests globally approximately 3% of the global forest area with tropical forests suffering the most severe damage, accounting for nearly 4% of the total burned area (FSI, 2021).

The persistence of hot and dry conditions, particularly over the wildlands and forest ecosystems, have caused extreme forest fire events (Duane *et al.,* 2021). At a global scale, North America, Southeastern Australia, and the Mediterranean region are the major hotspots of forest fire, which significantly experience extreme fire weather seasons (Cunningham *et al.,* 2024). In the recent decades, boreal and temperate conifer biomes were disproportionately affected due to increasing frequency and intensity of forest fires, affecting a significant human population (Cunningham *et al.,* 2024). Climate change has emerged as a key driver, amplifying global wildfire trends through increased temperatures, prolonged droughts, and more frequent heatwaves (Kreider *et al.,* 2024; Raymond *et al.,* 2020). The increase in global temperature driven by global warming has significantly increased the frequency, severity, and risk of forest fires, droughts, and heatwaves worldwide with India being no exception (Sun *et al.,* 2019; Chen *et al.,* 2024).

India's forests, which accounts for approximately 2% of the global forest area (about 80.9 million hectares or 24% of India's geographical area; FSI, 2021), predominantly consist of tropical evergreen, tropical deciduous, tropical montane and tropical thorn forests (FAO, 2012). Dry deciduous forests have been identified as highly fire-prone, especially during the pre-monsoon season (April–May) with approximately 65% of these forests classified as fire-susceptible zones (Sagar *et al.,* 2024). Notably, the northeastern and central regions of India are considered the most vulnerable to forest fires, with anthropogenic activities contributing to approximately 75% of the fire incidents in 2020 (WWF International, 2020). Over the local forest ecosystems, Uttarakhand fires have traditionally been perceived to be more devasting and harmful (Rawat *et al.,* 2017). Forest Fires are more trivial for developing countries with significant forest covers, as the damage to the ecosystems and the environment can be unprecedented. Indian forests have experienced significant forest fire event counts in past years (Kale *et al.,* 2017).

In India, certain species like Chir Pine (*Pinus roxburghii*) found in dry deciduous forests with broadleaf structures are particularly susceptible to fires in the Himalayan regions due to their high resin content in it (a highly flammable substance), which acts as a potent fuel source (Singh *et al.,* 2024; Bargali *et al.,* 2024). This susceptibility intensifies when soil moisture declines, vegetation senesces, and atmospheric dryness peaks (Sagar *et al.,* 2024). Additionally, the interplay of droughts and heatwaves intensifies the risk of forest fire by increasing fuel loads, especially in central India and adjacent regions, creating optimal conditions for ignition and rapid fire spread (Prabhakaran *et al.,* 2025).

Plant mortality from forest fires severely disrupts biodiversity and carbon storage, particularly in the topsoil. High-intensity fires deplete soil organic matter, alter pH, reduce nutrient availability, and destroy microbial communities, slowing nutrient cycling and vegetation recovery (Chandra *et al.,* 2015). Fire severity strongly influences biomass loss, with large, uncontrolled fires causing greater damage than low intensity burns (Keywood *et al.,* 2013; Neary *et al.,* 1999). Dense vegetation promotes surface-to-canopy fire spread, increasing destruction (Keith *et al.,* 2014). Repeated fires further degrade soil health, delay soil organic carbon (SOC) recovery (Xu *et al.,* 2022) and alter microbial communities affecting long-term vegetation succession and biomass structures (Stephens *et al.,* 2023).

In this context, the present study focuses on the 2022 forest fires in Uttarakhand – a critical event that underscores the vulnerability of Himalayan Forest ecosystems. The investigation aims to address two key research questions: 1) Do spatial observation datasets enhance our understanding of fire-induced changes in carbon and vegetation dynamics? and 2) How rapid was the post-fire ecosystem recovery? Through a detailed spatial-temporal analysis, this study explores how forest fire affects the biotic and abiotic components of the environment, particularly in the Uttarakhand region. Given that forest fires result from a complex interplay of environmental, atmospheric, and meteorological variables, the analysis integrates multiple datasets and approaches to unravel the sequential impacts of forest fires. Our work seeks to provide deeper insights into the formation of fire fuel loads, the extent of ecosystem damage, and the

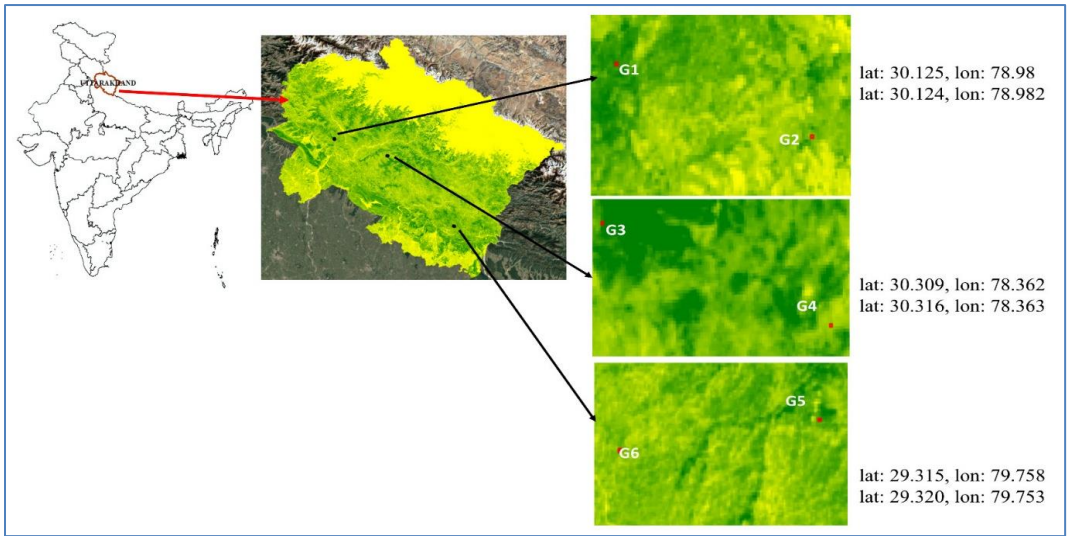

Fig. 1. Study area: parts of India, highlighting Uttarakhand for forest fire analysis. Multiple coloured boundary layers indicating the Zones for local scale analysis G1, G2, G3, G4, G5 & G6 made based on Dense and Sparse vegetation

potential pathways for ecosystem recovery and resilience following a forest fire.

2. Data and methodology

2.1. *Study area*

This study focuses on the 2022 Uttarakhand Forest fire event, examining the ecological impacts and recovery processes within the affected regions. Uttarakhand has approximately 45.6% of its geographical area covered with forest and dense vegetation, comprising nine major forest types: tropical moist deciduous forests, tropical dry deciduous forests, sub-tropical pine forests, Himalayan moist temperate forests, Himalayan dry temperate forests, sub-alpine forests, moist alpine scrub, dry alpine scrub, and tree outside forests (Bargali *et al.,* 2023). Fig. 1 illustrates the study area, where specific zones (G1, G2, G3, G4, G5 and G6) were delineated based on vegetation density (dense and sparse), with each zone covering a sample size of 100 m^2.

Key study locations include Chamba (elevation ~1,524 m), known for tree species like Albizia lebbeck, Ficus carica, Murraya koenigii, Quercus leucotrichophora, and Rhododendron arboreum (Himachal Pradesh State Biodiversity Board), and Dhanaulti, a temperate forested town where deodar, oak, rhododendron, and chir pine dominate across elevation gradients. Vegetation composition in these regions includes 13% trees, 19% shrubs, 7% climbers, and 61% herbs (Himachal Pradesh State Biodiversity Board, 2025). The study highlights how vegetation structure, soil moisture, and atmospheric conditions jointly influence the pace and magnitude of ecosystem recovery following fire disturbances.

2.2. *Data*

A combination of remote sensing datasets and meteorological observations was utilized to comprehensively assess the 2022 Uttarakhand Forest fire events. We used daily temperature and precipitation dataset from the India Meteorological Department (IMD) (Sharma *et al.,* 2024; Hari *et al.,* 2021) to deduce meteorological information including trends and spatial distribution, during the study period. The hourly (converted to 8-days temporal resolution for this study) data fifth generation of ECMWF atmospheric reanalysis (ERA5 Land) at ~9 km spatial resolution was used to monitor key soil and atmospheric variables, specifically soil moisture and vapor pressure deficit, providing insights into fuel conditions and fire susceptibility (Muñoz-Sabater *et al.,* 2021). Two fire products from the Moderate Resolution Imaging Spectroradiometer (MODIS) were used: the Fire Information for Resource Management System (FIRMS) with a 1 km spatial resolution for calculating fire counts and intensity, and the MCD64A1 Version 6.1 Burned Area data product with a 500 m spatial resolution for estimating the burned area (Campagnolo *et al.,* 2021). Additionally, three other MODIS products, including MCD12Q1.061 (Yearly Land Cover Type, 500 m), MOD17A2H (8-day Gross Primary Productivity, 500 m), and MOD16A2.061 (8-Day Net Evapotranspiration, 500 m) were used to determine the Land Use/Land Cover [LC_Type2, Annual University of Maryland (UMD) classification], Gross Primary Productivity (GPP), and Evapotranspiration (ET), respectively (Tithi *et al.,* 2024; Dong *et al.,* 2025). Furthermore, high spatio-temporal resolution data from Sentinel-2A (10 m, 20 m and 60 m spatial resolution, available at 10 - day interval) were used to derive the

TABLE 1

Data sources

Sl. No	Data Type	Variable /Products used	Temporal Resolution	Spatial Resolution	Data Source
1.	ERA5-Land (Reanalysis)	Soil Moisture, Vapour Pressure Deficit	Hourly	0.1° x 0.1° (9 km)	ECMWF
2.	Sentinel 2A	Soil Adjusted Vegetation Index (SAVI), Vegetation Condition Index (VCI), Leaf Area Index (LAI), kNDVI and reflectance bands	10 days	10 m	ESA
3.	MODIS: Fire Information for Resource Management System (FIRMS) and MCD64A1 Version 6.1	Fire Counts/Intensity and Burned area	Daily	1 km and 500 m	USGS
4.	MODIS: MODIS/061/MCD12Q1, MODIS/061/MOD17A2H and MODIS/061/MOD16A2	Land Use Land Cover, GPP and ET	Yearly (Annual), 8-day composite	500 m	USGS
5.	Indian Meteorological Department (IMD)	Maximum Temperature and Rainfall	Daily	1° and 0.25° respectively	IMD
6.	Global Ecosystem Dynamics Investigation (GEDI)	LiDAR data: aboveground biomass density	Monthly	25 m	ISS

indices to monitor vegetation dynamics caused by the forest fires. We estimated the above-ground biomass (AGB) density using the above-mentioned data variables, which was validated using LiDAR data acquired from the Global Ecosystem Dynamics Investigation (GEDI) (Francini *et al.*, 2022). A comprehensive list of the datasets used in this study are presented in Table 1.

2.2.1. *Vegetation Indices*

We used 10m resolution Sentinel-2A bands to derive various vegetation indices (Equations 1-5) to extract the vegetation-related parameters for the 2022 forest fire events in Uttarakhand. Specifically, we calculated the Soil-adjusted Vegetation Index (SAVI), Kernell Normalized Difference Vegetation Index (kNDVI), Enhanced Vegetation Index (EVI) (Lin *et al.*, 2019), Leaf Area Index (LAI), and Vegetation Condition Index (VCI) to assess the vegetation dynamics. Each index offers distinct advantages for capturing different aspects of vegetation conditions and characteristics. For example, SAVI effectively accounts for the influence of background soil information (*i.e.* reflectance) on vegetation areas, particularly in sparsely vegetated regions (Li *et al.*, 2018). The kNDVI is an advanced vegetation index that improves the detection of fine-scale vegetation regrowth and degradation following fire events (Li *et al.*, 2025). LAI provides information on the surface area of leaves per unit ground area, where higher values indicate greater moisture content and biomass, capturing the fuel load essential for evaluating pre- and post-fire vegetation conditions (Andalibi *et al.*, 2022; Djamai and Fernandes, 2018). Finally, VCI monitors heat and drought stress impacts on vegetation (Burka *et al.*, 2024), supporting the prediction of spatial and temporal variations in fire risk across the study area.

The indices computed from Sentinel 2A dataset are:

$$SAVI = (NIR+RED+L)/(NIR-RED)\times(1+L) \quad (1)$$

$$kNDVI = \tanh((NIR-Red)^2/(2\sigma)^2) \quad (2)$$

$$EVI = G * ((NIR - RED) / (NIR + C1 * RED - C2 * BLUE + L)) \quad (3)$$

$$LAI = 3.618 \times EVI - 0.118\text{-- }\ldots.. \quad (4)$$

$$VCI = (NDVI_{max}-NDVI_{min})/ (NDVI-NDVI_{min}) \times 100 \quad (5)$$

where, NIR: Near-Infrared reflectance, RED: Red reflectance, BLUE: Blue reflectance, σ: A scaling parameter that controls sensitivity to spectral difference. tanh: Hyperbolic tangent function to squash output to range ~ [0, 1). L: A soil brightness correction factor (typically around 0.5), which helps to adjust for soil effects, G= 2.5, C1= 6, C2= 7.5, L= 1.

2.2.2. *NBR, GPP, ET, PET, SH and LH*

Next, we used the Normalized Burnt Ratio (NBR) index to categorize and identify fires based on burn severity. NBR is the ratio of near-infrared and shortwave infrared bands (Equation 6) calculated using MODIS 8-day reflectance bands (MOD09A1.061). dNBR

from Equation 7, is calculated based on difference with Pre-fire NBR and Post-fire NBR image pixels.

$$NRB = ((NIR - SWIR) / (NIR + SWIR)) \quad (6)$$

$$dNBR = NBR_{pre\text{-}fire} - NBR_{post\text{-}fire} \quad (7)$$

We also estimated the total carbon fixed by vegetation through photosynthesis using the MODIS 8-day GPP product (Hari *et al.,* 2024). Similarly, integrated water loss from soil and plant transpiration was estimated using MODIS 8-day ET product, which helps in interpreting the health, potential and prolonged condition of fire fuel loads. These indicators reflect impaired vegetation function or slow forest ecosystem recovery, which can vary depending on vegetation type. Further, Vapour Pressure Deficit (VPD) and Soil Moisture (SM) were also derived from ERA5-Land product.

Daily potential evapotranspiration (PET; mm day^{-1}) was derived using the FAO-56 Penman-Monteith method, integrating INSAT surface insolation with three-hourly WRF meteorology (air temperature, humidity, wind speed), available at 5 km resolution (Bhattacharya *et al.,* 2009). We derived daily latent heat (LH, J/m²) and sensible heat (SH, J/m²) from ERA5-Land (Copernicus/ECMWF), accessed via GEE for the January 2022 to June 2025 period. We converted these daily totals to mean daily fluxes (W/m²) then harmonized sign to the micrometeorological convention (upward positive) and extracted for land-cover strata.

2.3. *Carbon density and biomass estimation*

Next, we derived the time-series of above-ground biomass (AGB), above-ground carbon (AGC), below-ground biomass (BGB), below-ground carbon (BGC), CO_2 sequestered in AGB, and total carbon (TC) stock over the forest ecosystem near Chamba district, Uttarakhand. The boundary was selected based on the fire affected patches. We used the machine learning (ML) models to make spatial AGB image and GEDI point data was used to validate. Random forest (RF), extra gradient boosting (XGBoost), decision tree and light gradient boosting (GBM) models were used to estimate AGB using Sentinel 2A data. The accuracy of selected ML models was benchmarked with the LiDAR-based monthly biomass data from GEDI.

The carbon (C) stock of the Himalayan Forests is a fraction of 47% of biomass (Dar and Parthasarathy, 2022). Therefore, AGC is calculated by multiplying the factor of conversion, as shown in Equation 8. The carbon-dioxide (CO_2) sequestration is estimated from the AGC using Equation 9 (Meragiaw *et al.,* 2021). Similarly, following the standard methods outlined by MacDicken (1997) and the IPCC (2006) report, and adopting a 5:1 shoot-to-root biomass ratio based on synthesized global data, belowground biomass (BGB) was estimated as 20% of aboveground biomass (AGB), as shown in Equation 10. For this study, total carbon (TC) stock was calculated by summing aboveground carbon (AGC) and BGB, following Pearson (2007). The TC stock (Mg ha^{-1}) for the study area is presented in Equation 11.

$$AGC = AGB * 0.47 \quad (8)$$

$$CO_{2\ sequestered}\_AGB = AGC \times 3.67 \quad (9)$$

$$BGB = AGB \times 0.20 \quad (10)$$

$$TC\ Stock = AGC + BGC \quad (11)$$

2.4. *Accuracy assessment*

The accuracy of the utilized models is assessed using mean squared error (MAE), root mean squared error (RMSE) and the coefficient of determination (R^2) metrics. RMSE and MAE metrics are used to evaluate the performance of ML models (Sunder *et al.,* 2023). The performance metrics are calculated using the equations (12 and 13) shown below:

$$RMSE = \sqrt{\frac{1}{n}\sum_{i=1}^{n}(\hat{y}_i - y_i)^2} \quad (12)$$

$$MAE = \frac{1}{n}\sum_{i=1}^{n}|\hat{y}_i - y_i| \quad (13)$$

3. Result and analysis

3.1. *Burn severity and intensity of the 2022 Uttarakhand forest fire*

First of all, we examined the fire burn severity of the 2022 forest fire in Uttarakhand using the Normalized Burnt Ratio (NBR). Since the fire was initiated in late February and persisted until the end of June, we estimated the NBR for two months in 2022 – January (pre-fire) and July (post-fire) over the burnt area, identified using MODIS Burnt Area products (MCD64A1). The pre-fire and post-fire NBR values were used to assess vegetation conditions before and after the fire Figs. 2(a & b). The difference between the pre- and post-fire NBR values (dNBR) was then used to estimate fire burn severity (Fig. 2c). The spatial distribution of NBR showed higher values (0.1 to 0.5), indicating relatively healthy vegetation condition before the fire (Fig. 2a). The NBR showed relatively low values (less than 0) in regions impacted by fire as compared to the pre-fire condition (Fig. 2b). As a

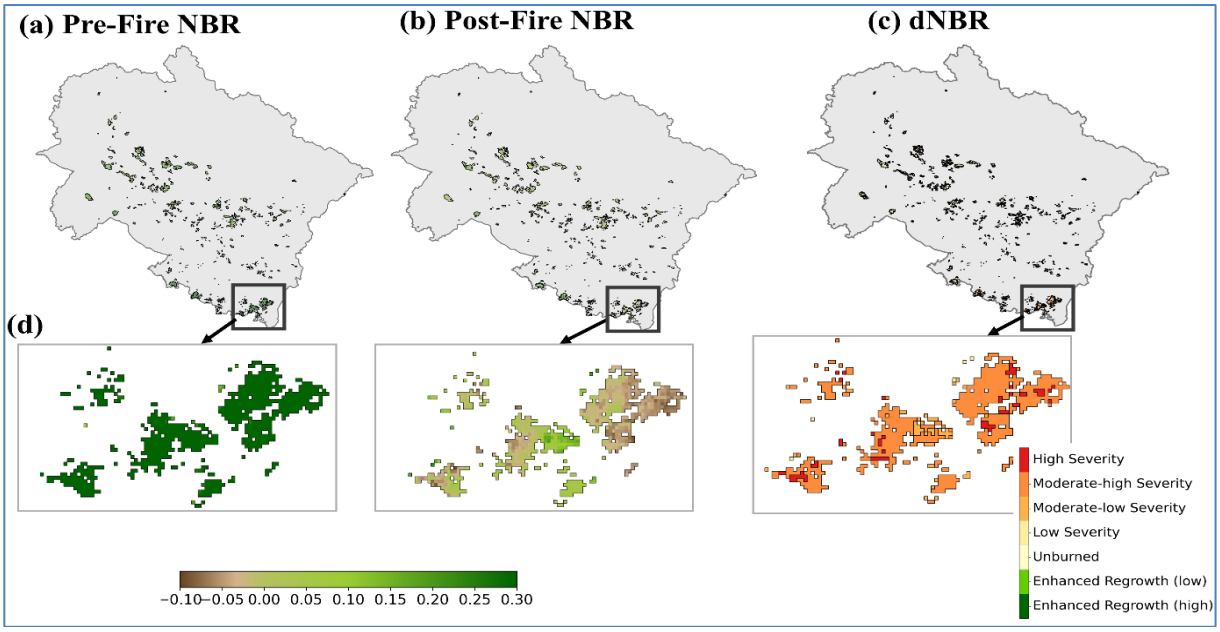

Figs. 2(a-d). NBR variation for (a) Pre-fire for Uttarakhand (b) Pre-fire for zoomed location (c) Post-fire for Uttarakhand (d) Post-fire for zoomed location

result, the dNBR also showed more negative values indicating greater vegetation loss due to the forest fire (Fig. 2c). To better interpret the results, we classified the dNBR values into different burn severity classes, including high, moderate-high, moderate-low, and low severity, along with unburned areas and zones of enhanced regrowth. Results revealed that most high-severity burns were concentrated in the southern parts of Uttarakhand, while moderate and low-severity impacts were more widespread. Pockets of enhanced regrowth, particularly in less severely affected areas, indicated early stages of secondary succession.

The NBR changes from per and post fires were also clear from the zoomed plots Figs. 2 (a & b) and had moderate to very high intensity of fire from Fig. 3. The intensity of the fires is classified from low to extreme based on the temperature of variations observed with the FIRMS fire data. The classifications have the lowest of 60 ºC and highest is 126.85 ºC. Nearly 2% of the Uttarakhand was burnt due to forest fire. The burnt area was mostly affected over the vegetated area when compared with LULC (supplementary Fig. S1). The burnt area covered 34.7% of woody savannas, 16% of savannas, 14% of mixed forest, 9.3% of Evergreen Needleleaf Forest, 1.7% of grasslands, 0.6% of Evergreen Broadleaf Forest and 0.13% of Deciduous Broadleaf Forest. The percentage difference of pre and post fire NBR values were observed to have 51.2% of evergreen need leaf forest, 48.5% of savannas, 40.4% of woody savannas, 36.9% of mixed forest, 32.7% of evergreen broadleaf forest, 12.3% of deciduous broadleaf forest and -17.7% grasslands (supplementary Fig. S2). The recovery of grasslands was observed to be very high could be possible due to the increase in monsoon rainfall. Since Uttarakhand's Forest ecosystem is frequently disturbed by extreme fire events (supplementary Fig. S3) and the health of these ecosystems can be monitored through biomass and carbon stock dynamics quantifying forest biomass and carbon stock loss was crucial.

3.2. *Biomass and carbon stock loss due to forest fires*

Next, we evaluated the biomass and carbon stock loss due to the forest fires in Uttarakhand during February-June 2022. The fire-affected area, along with its buffer region, covered approximately 219.97 km² (supplementary Figure S4a), which was then used to estimate the aboveground biomass (AGB), aboveground carbon (AGC), belowground biomass (BGB), belowground carbon (BGC), CO_2 in AGB, CO_2 in BGB, and total carbon (TC) stock. Our analysis revealed significant disruptions in biomass dynamics due to fire-induced changes in carbon pools (Figs. 4 & 5). The AGB was predicted using machine learning models (Random Forest, XGBoost, and LightGBM), where the Random Forest model performed best (R^2 = 0.74, RMSE = 145.9 Mg ha^{-1}, MAE = 103.5 Mg ha^{-1}). This model was used to estimate AGB from 2019 to 2022 (supplementary Figure S4) along with analysing feature importance of best predicted model (Random Forest) (supplementary Fig. S5), and we observed a clear reduction in 2022 compared to previous years, confirming the fire's impact on forest structure.

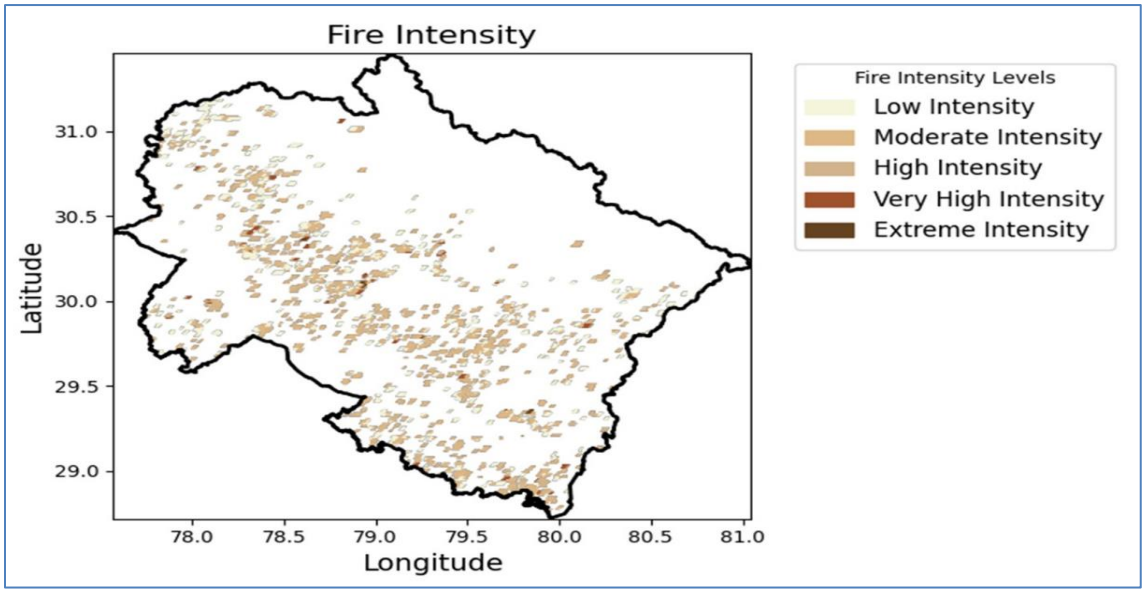

Fig. 3. Intensity levels of fire over the Uttarakhand study area

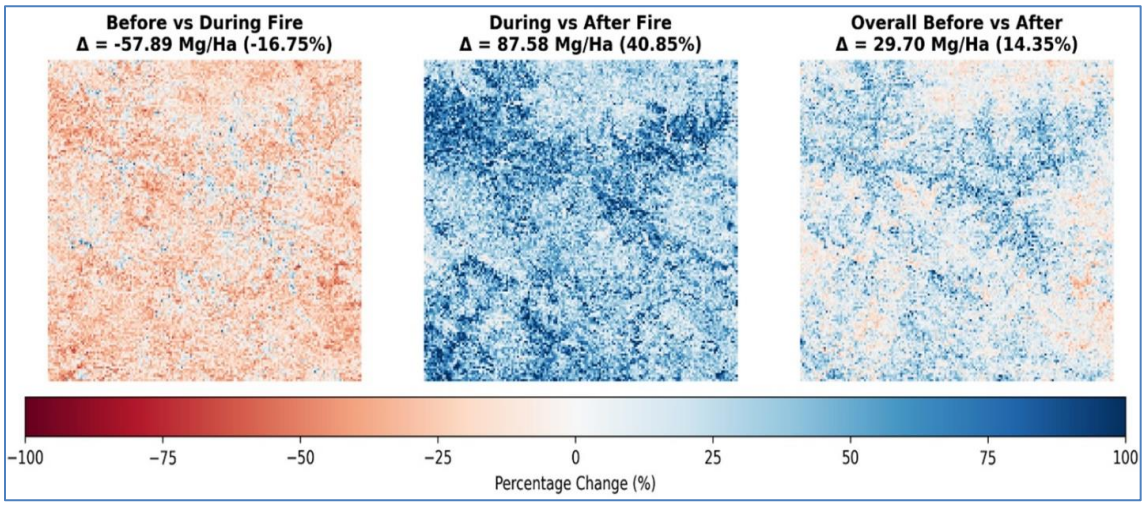

Fig. 4. Spatial and temporal percentage variation of AGB before, during and after the fire episodes over the fire patch buffer area

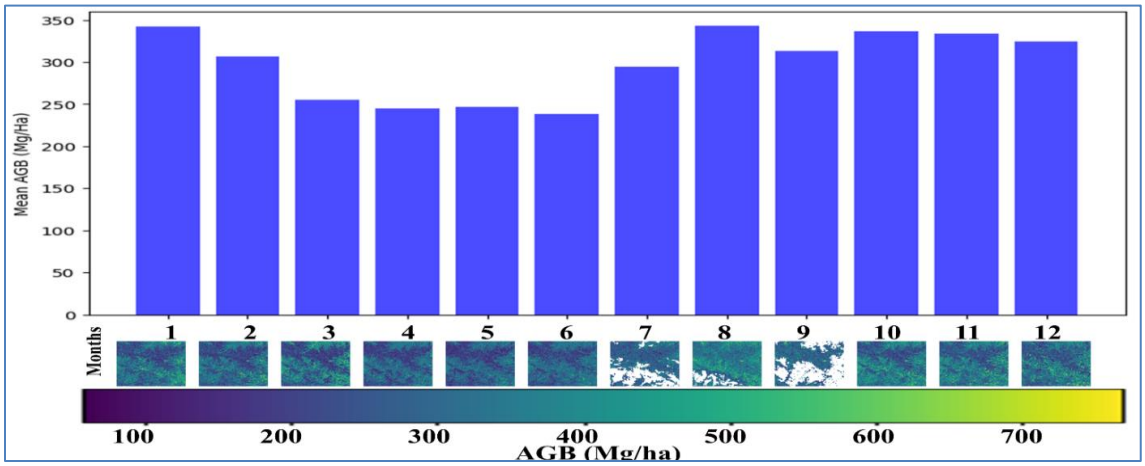

Fig. 5. Monthly AGB (Mg/ha) variation for year 2022 over the vicinity of fire patch

TABLE 2

Derived carbon stock pools in Mg/ha for AGB, AGC, BGB, BGC, CO_2 in AGB, CO_2 in BGB and TC stock over the Forest Fire ecosystem

Months	AGB	AGC	BGB	BGC	CO_2 in AGB	CO_2 in BGB	TC_Stock
Jan	404.60	202.30	80.92	40.46	742.44	148.49	242.76
Feb	388.90	194.45	77.78	38.89	713.64	142.73	233.34
Mar	325.03	162.51	65.01	32.50	596.42	119.28	195.02
Apr	303.43	151.72	60.69	30.34	556.80	111.36	182.06
May	268.70	134.35	53.74	26.87	493.07	98.61	161.22
Jun	263.06	131.53	52.61	26.31	482.72	96.54	157.84
Jul	406.54	203.27	81.31	40.65	746.00	149.20	243.93
Aug	410.72	205.36	82.14	41.07	753.66	150.73	246.43
Sep	415.66	207.83	83.13	41.57	762.73	152.55	249.39
Oct	366.77	183.39	73.35	36.68	673.03	134.61	220.06
Nov	393.48	196.74	78.70	39.35	722.03	144.41	236.09
Dec	407.09	203.55	81.42	40.71	747.02	149.40	244.26

Biomass loss was approximately 16%, aligning with the FIRMS observations of extreme fire intensities, where surface temperatures reached around 65 °C. Monthly variations in carbon pools (Table 2) and AGB (Figs. 4 & 5) showed a significant decline during the fire period (March–May), followed by a gradual recovery with the onset of the monsoon in June. A total AGB loss of 57.89 Mg ha^{-1} (16.75%) was recorded during the fire period, with biomass reduction and increased atmospheric carbon content occurring immediately after the fire. However, by July, the total carbon stock (AGC + BGC) recovered to near pre-fire levels, likely due to favourable conditions provided by the Indian summer monsoon.

We further observed a marked decline of approximately 230 Mg ha^{-1} in AGB between March and June, especially around Chamba in the Tehri Garhwal district. Although predicting carbon sinks is challenging, our estimates indicated that CO_2 sequestration capacity dropped from 596 Mg ha^{-1} to 482 Mg ha^{-1}, with corresponding total carbon stocks decreasing from 195 Mg ha^{-1} to 157 Mg ha^{-1}. Bargaili *et al.,* (2024) conducted an extensive study over biomass and carbon stock losses across Sal, Chir-Pine and mixed forests for 2022 fires and reported that high fire frequencies showed significant impact which make tree biomasses to decline and carbon stocks declined with the mean difference values by 12 Mg/ha-1 over Sal forest, mixed forests with 8 Mg/ha-1 and Chir-pine with 20 Mg/ha-1 stands being especially vulnerable due to species composition and fuel load. Sal forests showed greater resilience, particularly to low-intensity fires. The fire's impact was not limited to biomass, as soil carbon dynamics were also affected. Fires disrupted microbial communities in the soil, which are crucial for carbon sequestration and vegetation recovery. The disruption in microbial populations impacted nutrient cycling, making it harder for recovering vegetation to access essential nutrients like nitrogen and phosphorus. This highlighted the critical role microbial biomass plays in soil health and post-fire recovery.

The disturbance also revealed the differences in biomass sensitivity to fire, with AGB being more dynamic and affected than BGB, which is consistent with earlier studies (Mina *et al.,* 2023; Hari and Tyagi, 2022). AGB experienced a greater decline (32.35%) compared to BGB (32.48%). The total biomass loss during the fire period affected both aboveground and belowground carbon pools, with AGB and AGC seeing the largest reductions. Additionally, we found that repeated fires continued to disrupt the microbial biomass content (MBC) across soil depths, potentially delayed the recovery of soil organic carbon (SOC) for extended periods (Singh *et al.,* 2021; Xu *et al.,* 2022). The fire-induced disturbances also delayed soil recovery and microbial regeneration which further altered vegetation composition and community structure over the long term (Chanda, 2020).

In the post-fire period, we observed the early stages of secondary succession during the monsoon months. The charred biomass provided essential nutrients that facilitated microbial metabolism and soil carbon mineralization (Dooley *et al.,* 2012). As microbial communities recovered, they contributed to nutrient cycling, facilitating vegetation recovery. However, the long-term impacts of such disturbances on forest species' community composition and biomass structure remain a concern, as fire severity, coupled with climatic changes, could further alter ecosystem resilience and slow recovery. This study underscores the complexity of fire-induced changes to biomass and carbon stock, highlighting the importance of continuous monitoring for effective forest management and climate adaptation.

3.3. *Post-fire atmospheric recovery and its role in vegetation regrowth*

Next, we analysed the temperature and moisture dynamics during the 2022 forest fire period in Uttarakhand. Temperatures rose sharply during the initial phase, exceeding 40 °C and peaking above 45 °C, which contributed to increased atmospheric dryness and a higher frequency of fire events (Fig. S3). The VPD and SM, estimated from ERA5-Land data, exhibited an expected inverse relationship Figs. 6(a & b), highlighting intensified dryness from late February through June.

During June, a gradual increase in soil moisture (~0.2–0.4 $m^3 m^{-3}$) was observed across both dense and sparse vegetation classes (G1–G4). In contrast, G5 and G6 experienced a more rapid rise in SM beyond 0.4 $m^3 m^{-3}$, accompanied by a notable decrease in VPD below ~7 hPa, suggesting a strong coupling between atmospheric temperature and the upper soil layers. With the onset of rainfall in late May, as evident from IMD precipitation data (Fig. 6c), further increases in soil moisture and reductions in VPD were recorded, particularly over G5 and G6. VPD and SM are important factors that play a major role in the health of forest ecosystems, especially during the dry conditions (Mahto and Mishra, 2024; Rajeev *et al.,* 2022). They strongly influence how much water trees can use and how much carbon they can store (Cen *et al.*, 2025). During hot and dry periods, when VPD rises and SM falls, forests struggle to use water efficiently and to maintain their normal growth and carbon storage. These conditions also create an environment that allows fires to spread more easily.

After the fire events, the release of burnt plant material may have triggered a process called new particle formation (NPF). This process leads to the creation of extremely small, lightweight particles (ultrafine particles) in the air (Chen *et al.,* 2019). These particles are highly hygroscopic, meaning they attract water vapor easily, and they can serve as seeds for cloud formation (Wu *et al.*, 2017). This may have helped promote more rainfall over some forest areas in Uttarakhand after the fires. With the arrival of the monsoon season in June, rainfall became more frequent and intense. As a result, soil moisture levels increased steadily to about 0.4 to 0.5 $m^3 m^{-3}$, while VPD and air temperatures continued to decrease. This improvement in both land and atmospheric moisture is expected to play an important role in helping the forest vegetation recover after the fire damage.

3.4. *Post fire vegetation health recovery*

We further assessed the biophysical changes caused by the forest fire using high-resolution satellite data from Sentinel-2A. As shown in Fig. 7, a significant loss of vegetation greenness was observed across Uttarakhand during both the fuel accumulation period and the active fire season. This was detected using multiple vegetation indices, including SAVI, VCI, LAI, and kNDVI. During the initial fire phase, structural attributes of vegetation exhibited some inertia, delaying immediate response to environmental changes, while functional processes like energy and matter exchange showed quicker reactions. Functional vegetation traits, closely linked to nutrient cycling & carbon dynamics, can be effectively monitored to understand large-scale ecosystem responses to disturbance.

Wildfires directly disrupt ecosystem energy and matter flows, and tracking these changes provides insight into ecosystem dynamics and resilience. After June, SAVI values declined from ~0.4–0.5, indicating vegetation loss. Similarly, kNDVI values dropped sharply to near zero by May, reflecting significant vegetation degradation due to fire (Fig. 7d). Signs of recovery were observed from July onward, with VCI values increasing, suggesting post-fire vegetation regeneration. Following recovery initiation, VCI and LAI remained relatively stable and high between October and January, indicating restoration. However, heat and drought conditions during the fire period likely stressed vegetation further, enhancing canopy loss. Between June and September, vegetation dynamics fluctuated, reflecting post-fire ecological disturbances (Fig. 7).

Fire impacts on soil microbial communities depend on fire severity, changes in soil properties, and post-fire environmental conditions. By September, vegetation indices stabilized across the six sub-zones (G1-G6), with SAVI (~0.23-0.43), VCI (~40-80), LAI (~1-2), and kNDVI (~0.2-0.3), indicating recovery of vegetation health. Based on severity, fire disturbances are classified as: Degree 1: canopy, foliage, and branch destruction (Myers *et al.,* 2003), Degree 2: destruction of the canopy and understory, and Degree 3: damage extending to soil ecosystems and root structures (Nakagoshi & Touyama, 1995). Degree 3 disturbances require considerably longer recovery times compared to Degree 1 and 2. Vegetation indices such as kNDVI and LAI, sensitive to canopy cover, showed prolonged recovery or did not fully return to pre-fire levels within the short post-fire period, depending on fire severity. Thus, long-term monitoring is essential for a better understanding of ecosystem recovery processes following major fire events.

3.5. *Recovery of vegetation functionality: changes in GPP and ET*

Finally, we examined how forest fire has impacted the vegetation's evapotranspiration (ET) and carbon uptake

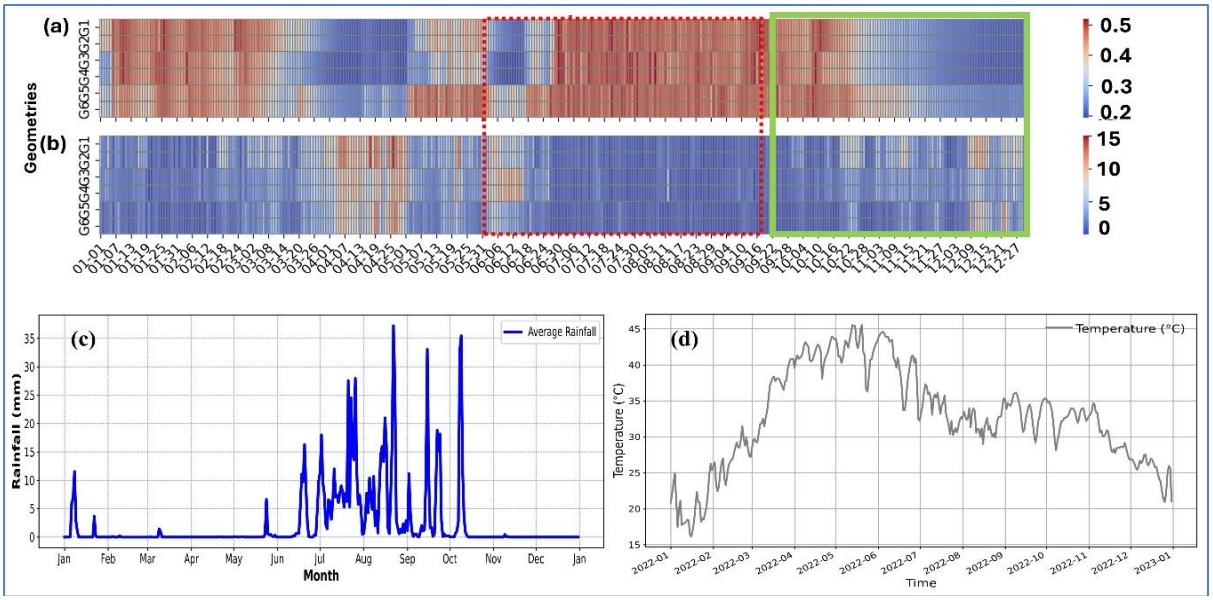

Figs. 6(a-d). Atmospheric condition of pre & post fire (a) SM (b)VPD for geometries (c) Rainfall (d) Maximum temperature for entire Uttarakhand

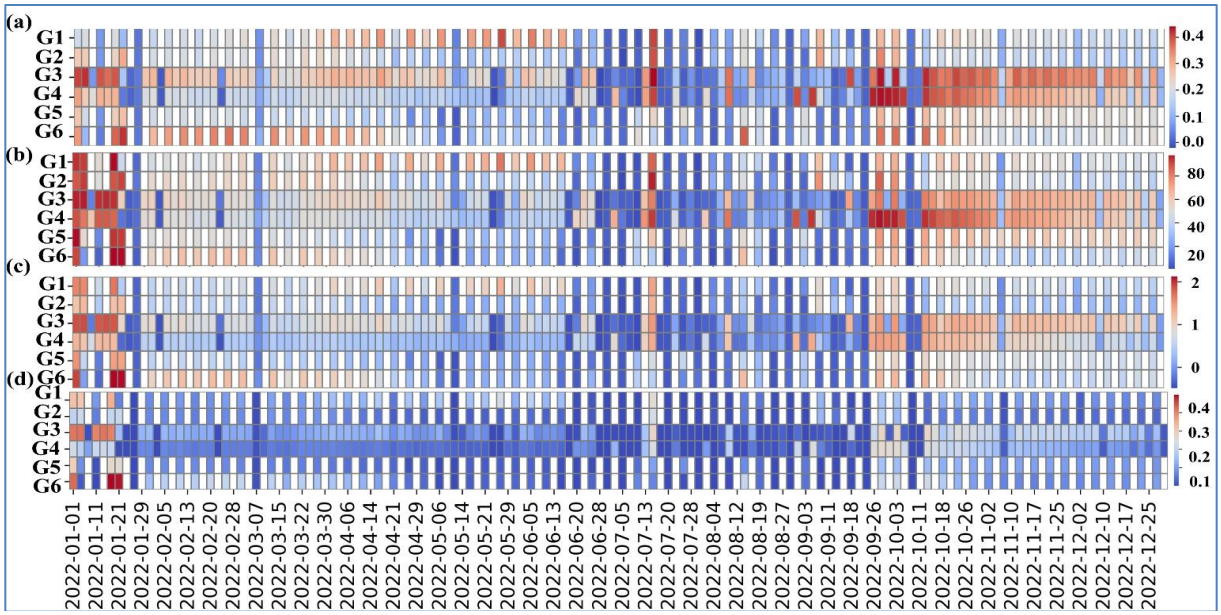

Figs. 7(a-d). Temporal Vegetation dynamics heat map using (a) SAVI (b) VCI (c) LAI (d) kNDVI for G1, G2, G3, G4, G5 and, G6 locations

(GPP) over the burned area's land cover types. We estimated the monthly ET and GPP anomaly for 2022-2024 over the burnt area for two vegetation types of Woody Savannas and Deciduous Forests and plotted against the significant (more than 10) fire counts (Fig. 8). Results show that GPP and ET significantly declined post-fire (June - July 2022) by approximately 20% and 13%, respectively. A similar pattern was observed in 2024, with reductions of around 20% in GPP and 12% in ET during the same post-fire window. Notably, vegetation appeared to take 1 - 2 months to exhibit the peak impact on both GPP and ET. A clear association was observed between the number of fire events and the reduction in GPP and ET (Shi *et al.*, 2025). The intense heat from the fires likely depleted vegetation water content, leading to physiological stress and, in many cases, vegetation mortality. Consequently, photosynthetic activity drastically declined, resulting in a substantial drop in GPP in the following months.

The internal characteristics of vegetation are analysed using GPP and ET. The concurrent or subsequent GPP reduction and ET are directly or indirectly linked to fire episodes. The decline of GPP and ET indicated the direct canopy loss and the decline of photosynthetic

Figs. 8(a&b). Vegetation internal characteristics (a) GPP (b) ET for woody savannas and deciduous broadleaf forests along with fire counts for burnt area

activity with fewer active leaves. It also highlights the sensitivity of ecosystem productivity and water fluxes to fire disturbances. The lag in response further suggests a cumulative or delayed effect of fire damage, possibly driven by post-fire vegetation recovery dynamics and soil moisture depletion. This also creates loss of transpiration structural damage, and stomatal dysfunction suppresses ET (Shi *et al.*, 2025). Due to thermal stress or desiccation and as GPP is coupled with carbon and water fluxes, fire disturbances over the ecosystem have limited the CO_2 uptake and caused GPP to decline. Spatial analysis also revealed that regions with higher fire density experienced more pronounced reductions, indicating a strong spatial heterogeneity in fire impacts (Hemes *et al.*, 2023).

When the canopy is reduced, the interception and changes in energy balance potentially increase evaporation temporarily but significantly reduce transpiration dominance in ET. A decline in ET due to fire as a feedback loop could alter VPD or other microclimatic factors (Zhou *et al.*, 2014), exacerbating stomatal closure and further reducing GPP. The effects of hydrophobic soil layers could be more severe, further limiting water uptake and affecting both plant water use (ET) and carbon assimilation (GPP). This can also lead to a lagged GPP response even after ET drops due to slow metabolic regrowth, consistent with the lagged correlation, resulting in the strongest GPP suppression one day after the fire episode. These findings underscore the importance of fire monitoring and post-fire recovery assessment in managing ecosystem resilience under changing climate conditions.

3.6. *Sub-seasonal recovery and intricate relationship with PET, ET, LH, and SH*

Wildfires intensely altered the land atmosphere energy exchange and water balance, modifying vegetation canopy structure, soil moisture availability, soil surface roughness and temperature gradients between surface and air. To assess short term biophysical impact due to peak fires with the atmospheric moisture demand and surface energy, we analysed anomalies of four key surface flux variables PET, ET, SH, and LH across two dominant vegetation classes in Uttarakhand (Woody Savannas and Deciduous Broadleaf Forests) during fire-impacted days (fire_pixel_count > 10), considering the time windows spanning pre-fire to post-fire conditions. The variations are shown in Figs. 9(a-c). Increase in fires suppressed the ET levels from vegetation, which was aligned with the anticipated physiological stress and loss of green biomass followed by intense fire activity. This inability of vegetation's to transpire effectively during and shortly after fire events was linked with stomatal closure, leaf area loss, and post-fire canopy mortality.

During the early dry season of fire, April to May 2022, the results showed significant gradual decline of ET, notably, 15.5% in Woody Savannas and 8.2% in Deciduous Forests, which reflected the immediate effect over vegetation suppression due to stomatal closure, canopy loss and foliar scorching. Despite of ET, the PET increased around 19% in Woody Savannas and 17.5% in Deciduous Forest, which clearly decoupled the relation between atmospheric evaporative demand and ecosystem water supply. This divergence of ET and PET explained the

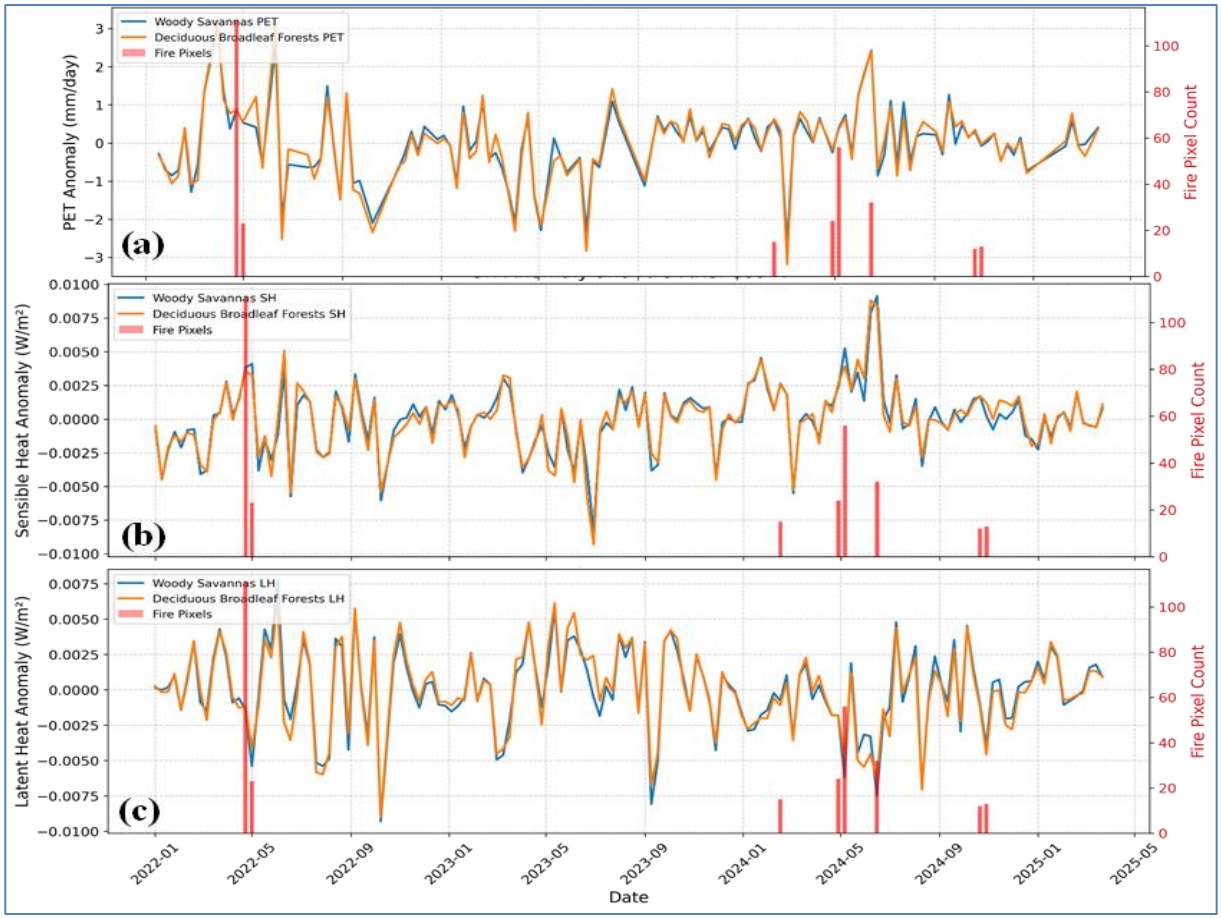

Figs. 9(a-c). Vegetation internal characteristics (a) PET (b) SH and (c) LH for woody savannas and deciduous broadleaf forests along with fire counts for burnt area

increased aridity, whereas, land surfaces energies became limited due to reduced moisture exchange. The surface energy balance showed impeccable evidence of post – fire partitioning shifts. The LH (the energy flux associated with evapotranspiration) decreased after fire up to 26.1% and 20.9% in Woody Savannas and Deciduous Forests, respectively, followed the patterns of ET. This suppression of LH indicated reduced capacity of the surface to dissipate heat via latent cooling, directly affecting surface energy dissipation and boundary layer stability. In tandem, SH increased by 50.2% and 45.4% in Woody Savannas and Deciduous Forests, respectively, signalling a reallocation of available net radiation towards atmospheric heating of the lower tropospheric atmosphere, which critically altered the land atmosphere energy coupling.

The fire windows, when extended to 2024 dry pre-monsoon seasons (February to May) considering multiple fire occurrences, the ET declined further than in 2022 fire event, with 18.0% in Woody Savannas and 14.4% in Deciduous Forests. This reflected a strong interpretation of compound stress impact over the vegetation due to long and intense exposure of fires. Interestingly, PET anomalies during this event were more modest (6.7%, 6.8%) with the 5-day threshold of post fire, possibly due to seasonal moderation of atmospheric demand. Nonetheless, the consistent rise again highlighted the increasing atmospheric water demand amidst falling biological water fluxes which is a signature of fire-induced hydroclimatic imbalance. LH remained negatively impacted (22.4%, 20.2%), confirming persistent declines in evaporative surface cooling whereas SH rose substantially (43.3%, 40.9%), this echoed earlier findings of thermal amplification in post-burns and reinforced the positive feedback loop between fire, dryness, and surface heating.

Moreover, the fires on post monsoon during October revealed distinct seasonal responses. The divergence of ET (9.5%, 20.8%) and PET (3.0%, 3.8%) suggested significant resilience, whereas dense forest types were found comparatively vulnerable. The decoupling between PET and ET anomalies exemplified a transition from energy-limited to moisture-limited evapotranspiration regimes during fire-affected months. This shift has showed direct implications for drought intensification, vegetation recovery lags, and future fire susceptibility. As expected,

the energy partitions remained consistent with previous pattern with LH, showed decline of 19.1% and 22.5% and SH had increased variation of about 11.9% and 19.4%, highlighted the reinforced dominance of SH even under the milder meteorological conditions.

This setback of LH and SH dominance on post-fire period is a benchmark of fire-disturbed systems, where vegetation loss and topsoil exposure increase the albedo and reduce the surface moisture buffer. The observed increase in SH more likely accelerated the land atmosphere coupling strength and daytime boundary layer growth, that potentially resulted altering the local convective dynamics and precipitation initiation (Mölders and Kramm, 2007; Dirmeyer *et al.,* 2014). The fires impacts showed uneven response over the biomes', especially with the higher SH in Woody Savannas showed greater surface desiccation and radiative stress in these ecosystems, possibly due to less structural resistance to fire (Jhariya and Raj, 2014). The synergy between reduced LH and increased SH can generate localized surface warming (positive feedback), which, in turn, could exacerbate fuel drying and trigger recurrent fire cycles especially in already vulnerable forest types like pine-dominated savannas (Liu *et al.,* 2019; Beringer *et al.,* 2007).

4. Conclusions

The recovery analysis of the 2022 forest fire events provides insights into the restoration trajectory of degraded vegetation across Uttarakhand. The 2022 fire episodes made significant destruction of vegetation ecosystem. The fire counts over the Uttarakhand region were witnessed from late February to June. Moreover, the increase in the number of fire counts was observed from April to early June summer months. The increase in the number of fires counts along with the atmospheric dryness has decreased vapor pressure deficit and top-level soil moisture levels over the ecosystem. The results indicated that during periods of elevated temperature, all vegetation-related indices including SAVI, VCI, kNDVI, and LAI exhibited significant declines, reflecting acute vegetation stress, loss of canopy cover, and heightened fire susceptibility. This implied that the Uttarakhand Forest ecosystem was vulnerable to fires, with the most burnt across the forest covers by woody savannas, savannas and mixed forest. Among the five vegetation indicators, kNDVI responded earliest, capturing early signs of vegetation degradation before visible loss, thereby highlighting its potential for early warning applications.

The post-fire monitoring through vegetation indices suggests that significant vegetation recovery marked by stabilization of VCI, SAVI, kNDVI, and LAI began approximately 3 to 4 months after the fire event, particularly noticeable from September onwards due to the Indian summer monsoon rainfall. However, full restoration of pre-fire vegetation structures, especially in severely burnt zones, is likely to require multiple years, depending on fire severity, soil conditions, and climatic factors. Satellite-based indices revealed evidence of secondary succession, characterized by the proliferation of fast-growing shrubs and grasses in the post-fire period. This suggests an initial phase of ecosystem reorganization rather than immediate recovery of original forest types. Species like Chir Pine and Sal, which are more fire-adapted, appeared to expand into areas previously dominated by Oak forests, potentially driving long-term shifts in ecosystem composition and function.

Internal vegetation dynamics from 2022 to 2024 revealed a 20% decline in GPP and a 13% reduction in ET during the immediate post-fire period of 2022. A similar magnitude of decline (20% for GPP and 12% for ET) was recorded in 2024, reflecting the compounded impacts of repeated fire events. Recurrent fires were found to delay the recovery period and hinder ecosystem functional stability. Additionally, assessments of carbon pools including AGB, BGB, and their associated carbon stocks emphasized significant reductions before, during, and after the fire episodes, further affecting the carbon sequestration potential of the forest ecosystem.

Post-fire burned regions showed coherent hydro-biophysical shifts, with showed decline in GPP (~20%) and ET (8-21%), while PET increased up to 3-19%, which signalled stronger atmospheric moisture demand against weakened moisture supply. These shifts were interlinked with the surface energy partitioning, which was reallocated from latent (19-26%) to sensible heating (12–50%), which explained the reduced evaporative cooling and enhanced near-surface warming. Woody Savannas exhibited the strongest thermal amplification, with SH > +40% during fire windows. Deciduous Broadleaf Forests showed deeper ET deficits (−21%), the consistent with canopy scorch, suppressed transpiration rate. The PET-ET divergence revealed moisture demand and supply decoupling, that was significantly observed immediately after fires, which explained hallmark of moisture-limited conditions.

Peak impacts emerged within days of ignition and persisted through the buffered post-fire period across both land cover types. Where SH > +40% co-occurred with LH < −20%, recovery was slowest, indicating strong energy reallocation and soil canopy dryness. Coupled water, energy, carbon signals (ET/LH down, SH/PET up, GPP down) diagnose constrained vegetation function and limited cooling capacity. These changes intensified the boundary-layer growth and local heat stress, reinforcing fire climate feedback. Management needs to reconsider the

prioritized hotspots crossing the SH/LH thresholds above, as they represent high-risk, slow-recovery patches.

With rising global temperatures, climatic changes such as drought and heatwaves are expected to increase fire frequency with shorter return intervals (Mina *et al.,* 2023; Tepley *et al.*, 2018; Kumar *et al.,* 2023). When forests are repeatedly disturbed before full recovery, ecosystem resilience diminishes, making them more vulnerable to future disturbances. Over time, this can shift ecosystems toward critical tipping points, leading to shorter recovery cycles and reduced resistance and resilience among tree species (Thom, 2023).

Overall, the study highlights that satellite observations are effective for large-scale, rapid assessments of post-fire recovery. Our findings underscore the urgent need for proactive fire management and post-fire restoration strategies to enhance forest resilience under changing climate conditions. Moreover, continuous long-term monitoring is essential to distinguish between genuine forest recovery and shifts toward alternate vegetation states triggered by fire disturbances.

Data Availability Statement

The ERA5 data used in the present study are obtained from the website (https://cds.climate.copernicus.eu/datasets /reanalysis-era5-single-levels?tab=download).

Acknowledgements

The authors would like to acknowledge the National Institute of Technology Rourkela for providing lab facilities. We also extend our gratitude to IMD for providing temperature and precipitation datasets, ECMWF for access to essential climate modelling data, Copernicus for high resolution datasets and MODIS for satellite imagery and datasets. These resources have been invaluable in supporting our research. BT wants to acknowledge the Ministry of Earth Sciences (MoES), Government of India, for the sponsored research grant, valuable for conducting research for the present work.

Authors' Contributions

M.S. Shyam Sunder: writing – original draft preparation, visualization; writing- review and editing.
Shanti Shwarup Mahto: writing – review, and editing; visualization.
Bhishma Tyagi: Conceptualization, writing – original draft preparation, writing – review, and editing, supervision,
All the authors have read and approved the final manuscript.

Disclaimer: The contents and views presented in this research article/paper are the views of the authors and do not necessarily reflect the views of the organizations they belong to.

References

Andalibi, L., Ghorbani, A., Darvishzadeh, R., Moameri, M., Hazbavi, Z., Jafari, R. and Dadjou, F., 2022, "Multisensor assessment of leaf area index across ecoregions of Ardabil Province, northwestern Iran", *Remote Sens.*, **14**, 22, 5731. https://doi.org/ 10.3390/rs14225731.

Bargali, H., Bhatt, D., Sundriyal, R.C., Uniyal, V.P., Pandey, A. and Ranjan, R., 2023, "Effect of forest fire on tree diversity and regeneration in the forests of Uttarakhand, Western Himalaya, India", *Front. For. Glob. Change*, **6**, 1198143. https://doi.org/ 10.3389/ffgc.2023.1198143

Bargali, H., Pandey, A., Bhatt, D. and Sundriyal, R.C., 2024. "Loss of carbon stock in the forests of Uttarakhand due to unprecedented seasonal forest fires". *Front. For. Glob. Change.*, **7**, 1352265. https://doi.org/10.3389/ffgc.2024.1352265

Beringer, J., Hutley, L.B., Tapper, N.J. and Cernusak, L.A., 2007, "Savanna fires and their impact on net ecosystem productivity in North Australia", *Glob. Change Biol.*, **13**, 5, 990-1004. https://doi.org/10.1111/j.1365-2486.2007.01334.x

Bhattacharya, B.K., Mallick, K., Padmanavan, N., Patel, N.K. and Parihar, J.S., 2009, "Simple retrieval of land surface albedo and temperature using data from Indian geostationary satellite - a case study for winter months", Intern. J. Remote Sens., 30, **12**, 3239–3257. https://doi.org/10.1080/01431160802559061

Burka, A., Biazin, B. and Bewket, W., 2024, "Spatial drought occurrences and distribution using VCI, TCI, VHI, and Google Earth Engine in Bilate River Watershed, Rift Valley of Ethiopia", Geomatics Nat. Hazards Risk, **15**, 1, 2377672. https://doi.org/10.1080/ 19475705.2024.2377672

Campagnolo, M.L., Libonati, R., Rodrigues, J.A. and Pereira, J.M.C., 2021, "A comprehensive characterization of MODIS daily burned area mapping accuracy across fire sizes in tropical savannas", *Remote Sens. Environ.*, **252**, 112115. https://doi.org/ 10.1016/j.rse.2020.112115

Chanda, S., 2020. "Study of soil micro-organisms under Chir Pine Forest in post fire conditions at Purola Range Of Uttarakhand". *Environ. Sci.*, **7**, 5, 8.

Chandra, K.K. and Bhardwaj, A.K., 2015, "Incidence of forest fire in India and its effect on terrestrial ecosystem dynamics, nutrient and microbial status of soil", *Int. J. Agric. For.*, **5**, 2, 69–78. DOI: 10.5923/j.ijaf.20150502.01

Cen, Y., Tang, M., Wang, Q., Sun, G., Han, Z., Li, Y. and Gao, Z., 2025, "Vapor pressure deficit dominates dryness stress on forest biomass carbon in China under global warming", *Agric. For. Meteorol.*, **364**, 110440. https://doi.org/10.1016/j.agrformet. 2025.110440.

Chen, L., Li, Q., Wu, D., Sun, H., Wei, Y., Ding, X., Chen, H., Cheng, T. and Chen, J., 2019, "Size distribution and chemical composition of primary particles emitted during open biomass burning processes: Impacts on cloud condensation nuclei activation", *Sci. Total Environ.*, **674**, 179–188. https://doi.org/10.1016/ j.scitotenv.2019.03.419.

Chen, S., Stark, S.C., Nobre, A.D., Cuartas, L.A., de Jesus Amore, D., Restrepo-Coupe, N., Smith, M.N., Chitra-Tarak, R., Ko, H., Nelson, B.W. and Saleska, S.R., 2024, "Amazon forest biogeography predicts resilience and vulnerability to drought",

Nature, **631**, 8019, 111–117. https://doi.org/10.1038/s41586-024-07568-w.

Cunningham, C.X., Williamson, G.J. and Bowman, D.M., 2024, "Increasing frequency and intensity of the most extreme wildfires on Earth", *Nat. Ecol. Evol*., **8**, 1–6. https://doi.org/10.1038/s41559-024-02452-2.

Dar, A.A. and Parthasarathy, N., 2022, "Patterns and drivers of tree carbon stocks in Kashmir Himalayan forests: implications for climate change mitigation", *Ecol. Process.*, **11**, 1, 58. https://doi.org/10.1186/s13717-022-00402-z.

Dirmeyer, Paul A., Zaiyu Wang, Mbongowo J. Mbuh, and Holly E. Norton, 2014. "Intensified land surface control on boundary layer growth in a changing climate." *Geophys. Res. Lett.*, **41**, 4, 1290-1294. https://doi.org/10.1002/2013GL058826.

Djamai, N. and Fernandes, R., 2018, "Comparison of SNAP-derived Sentinel-2A L2A product to ESA product over Europe", *Remote Sens.*, **10**, 6, 926. https://doi.org/10.3390/rs10060926.

Dong, W., Yuan, H., Lin, W., Liu, Z., Xiang, J., Wei, Z., Li, L., Li, Q. and Dai, Y., 2025, "A global urban tree leaf area index dataset for urban climate modeling", *Sci. Data*, **12**, 1, 426. https://doi.org/10.1038/s41597-025-04729-y.

Dooley, S.R. and Treseder, K.K., 2012, "The effect of fire on microbial biomass: a meta-analysis of field studies", *Biogeochemistry*, **109**, 49–61. https://doi.org/10.1007/s10533-011-9633-8.

Duane, A., Castellnou, M. and Brotons, L., 2021, "Towards a comprehensive look at global drivers of novel extreme wildfire events", *Clim. Change*, **165**, 3, 43. https://doi.org/10.1007/s10584-021-03066-4.

Francini, S., D'Amico, G., Vangi, E., Borghi, C. and Chirici, G., 2022, "Integrating GEDI and Landsat: Spaceborne lidar and four decades of optical imagery for the analysis of forest disturbances and biomass changes in Italy", *Sensors*, **22**, 5, 2015. https://doi.org/10.3390/s22052015.

FAO, 2012, "INDIA FORESTRY OUTLOOK STUDY", Food and Agriculture Organization of the United Nations, Rome. https://www.fao.org/4/am251e/am251e00.pdf. (Accessed: 1 January 2025).

FSI, 2021, "India State of Forest Report 2021", Forest Survey of India, https://www.fsi.nic.in/forest-report-2021.

Hari, M., Kutty, G. and Tyagi, B., 2024. "Integrating multi-source datasets in exploring the covariation of gross primary productivity (GPP) and solar-induced chlorophyll fluorescence (SIF) at an Indian tropical forest flux site", *Environ. Earth Sci.*, **83,** 8, 232. https://doi.org/10.1007/s12665-024-11528-y.

Hari, M. and Tyagi, B., 2022, "Terrestrial carbon cycle: tipping edge of climate change between the atmosphere and biosphere ecosystems", *Environmental Science: Atmospheres*, **2,** 5, 867-890. https://doi.org/10.1039/D1EA00102G.

Hari, M., Srinivasan, S., Rajasekaran, A. and Tyagi, B., 2021, "Above ground carbon stock mapping over Coimbatore and Nilgiris Biosphere: A key source to the C sink", *Carbon Manag.*, **12**, 4, 411–428. https://doi.org/10.1080/17583004.2021.1962979.

Hemes, K.S., Norlen, C.A., Wang, J.A., Goulden, M.L. and Field, C.B., 2023. The magnitude and pace of photosynthetic recovery after wildfire in California ecosystems. *Proc. Natl. Acad. Sci. U. S. A.*, **120**, 15, 2201954120. https://doi.org/10.1073/pnas.2201954120.

Himachal Pradesh State Biodiversity Board, 2025, "Tree species found in Chamba", HP Biodiversity Board, https://hpbiodiversity.gov.in/Pdf/tree%20species%20found%20in%20%20Chamba.pdf (Accessed: 25 March 2025).

IPCC (Intergovernmental Panel on Climate Change), 2006, "Guidelines for national greenhouse gas inventories. Volume 4", IGES Publishing, Hayama, Japan.

Jhariya, M.K. and Raj, A., 2014. "Effects of wildfires on flora, fauna and physico-chemical properties of soil-An overview", *J. Appl. Nat. Sci.*, **6**, 2, 887.

Jones, M.W., Abatzoglou, J.T., Veraverbeke, S., Andela, N., Lasslop, G., Forkel, M., Smith, A.J., Burton, C., Betts, R.A., van der Werf, G.R. and Sitch, S., 2022, "Global and regional trends and drivers of fire under climate change", *Rev. Geophys.*, **60**, 3, e2020RG000726. https://doi.org/10.1029/2020RG000726

Kale, M.P., Ramachandran, R.M., Pardeshi, S.N., Chavan, M., Joshi, P.K., Pai, D.S., Bhavani, P., Ashok, K. and Roy, P.S., 2017, "Are climate extremities changing forest fire regimes in India? An analysis using MODIS fire locations during 2003–2013 and gridded climate data of India meteorological department", *Proc. Natl. Acad. Sci. India A Phys. Sci.*, **87**, 827–843. https://doi.org/10.1007/s40010-017-0452-8

Keith, H., Lindenmayer, D.B., Mackey, B.G., Blair, D., Carter, L., McBurney, L., Okada, S. and Konishi-Nagano, T., 2014, "Accounting for biomass carbon stock change due to wildfire in temperate forest landscapes in Australia", *PLoS One*, **9**, 9, e107126. https://doi.org/10.1371/journal.pone.0107126.

Keywood, M., Kanakidou, M., Stohl, A., Dentener, F., Grassi, G., Meyer, C.P., Torseth, K., Edwards, D., Thompson, A.M., Lohmann, U. and Burrows, J., 2013, "Fire in the air: Biomass burning impacts in a changing climate", *Crit. Rev. Environ. Sci. Technol.*, **43**, 1, 40–83. https://doi.org/10.1080/10643389.2011.604248.

Kreider, M.R., Higuera, P.E., Parks, S.A., Rice, W.L., White, N. and Larson, A.J., 2024, "Fire suppression makes wildfires more severe and accentuates impacts of climate change and fuel accumulation", *Nat. Commun.*, **15**, 1, 2412. https://doi.org/10.1038/s41467-024-46702-0.

Kumar, P., Patel, A., Rai, J. and Kumar, P., 2023. "Environmental challenges and concurrent trend of weather extremes over Uttarakhand Himalaya". *Theor. Appl. Climatol.*, **155**, 2, 1217-1246. https://doi.org/10.1007/s00704-023-04690-z.

Li, G., Lai, H., Chen, B., Yin, X., Kou, W., Wu, Z., Chen, Z. and Wang, G., 2025, "Spatial distribution pattern of forests in Yunnan Province in 2022: Analysis based on multi-source remote sensing data and machine learning", *Remote Sens*., **17**, 7, 1146. https://doi.org/10.3390/rs17071146.

Li, C., Zhu, X., Wei, Y., Cao, S., Guo, X., Yu, X. and Chang, C., 2018, "Estimating apple tree canopy chlorophyll content based on Sentinel-2A remote sensing imaging", *Sci. Rep.*, **8**, 1, 3756. https://doi.org/10.1038/s41598-018-21963-0.

Lin, S., Li, J., Liu, Q., Li, L., Zhao, J. and Yu, W., 2019, "Evaluating the effectiveness of using vegetation indices based on red-edge reflectance from Sentinel-2 to estimate gross primary productivity", *Remote Sens.*, **11**, 11, 1303. https://doi.org/10.3390/rs11111303.

Liu, Z., Ballantyne, A.P. and Cooper, L.A., 2019, "Biophysical feedback of global forest fires on surface temperature", *Nat. Commun.*, **10**, 1, 214. https://doi.org/10.1038/s41467-018-08237-z.

Mahto, S.S. and Mishra, V., 2024, "Flash drought intensification due to enhanced land–atmospheric coupling in India", *J. Clim.*, **37**, 20, 5291–5307. https://doi.org/10.1175/JCLI-D-22-0477.1.

Mina, U., Dimri, A.P. and Farswan, S., 2023, "Forest fires and climate attributes interact in central Himalayas: an overview and assessment", *Fire Ecol.*, **19**, 1, 1–18. https://doi.org/10.1186/s42408-023-00177-4.

Muñoz-Sabater, J., Dutra, E., Agustí-Panareda, A., Albergel, C., Arduini, G., Balsamo, G., Boussetta, S., Choulga, M., Harrigan, S., Hersbach, H. and Martens, B., 2021, "ERA5-Land: A state-of-the-art global reanalysis dataset for land applications", *Earth Syst. Sci. Data*, **13**, 9, 4349–4383. https://doi.org/10.5194/essd-13-4349-2021

Myers, P.E. and Davis, J.S., 2003, "Recolonization of soils by algae in a north central Florida pine forest after controlled fire and soil sterilization", *Nova Hedwigia*, **76**, 207–219. https://doi.org/10.1127/0029-5035/2003/0076-0207.

Nakagoshi, N. and Touyama, Y., 1995, "Disturbances and recovery processes of a pine forest ecosystem in a fire regime", *J. Int. Dev. Coop.*, **1**, 43–59.

MacDicken, K.G., 1997, "A guide to monitoring carbon storage in forestry and agroforestry projects", *Winrock Int*, Arlington, Virginia.

Meragiaw, M., Woldu, Z., Martinsen, V. and Singh, B.R., 2021, "Carbon stocks of above- and belowground tree biomass in Kibate Forest around Wonchi Crater Lake, Central Highland of Ethiopia", *PLoS One*, **16**, 7, e0254231. https://doi.org/10.1371/journal.pone.0254231.

Mölders, N. and Kramm, G., 2007. "Influence of wildfire induced land-cover changes on clouds and precipitation in Interior Alaska—A case study". *Atmos. Res.*, **84**, 142-168. https://doi.org/10.1016/j.atmosres.2006.06.004.

Neary, D.G., Klopatek, C.C., DeBano, L.F. and Ffolliott, P.F., 1999, "Fire effects on belowground sustainability: a review and synthesis", *For. Ecol. Manage.*, **122**, 1–2, 51–71. https://doi.org/10.1016/S0378-1127(99)00032-8.

Prabhakaran, A. and Srivastava, P., 2025, "Analysis of prevailing atmospheric conditions during wildfire events in the Indian Himalayan region", *Q. J. R. Meteorol. Soc.*, **151**, 767, e4918. https://doi.org/10.1002/qj.4918.

Pearson, T.R., 2007, "Measurement guidelines for the sequestration of forest carbon", U.S. Dep. Agric. For. Serv. North. Res. Stn., **18**.

Rajeev, A., Mahto, S. S., & Mishra, V., 2022, "Climate warming and summer monsoon breaks drive compound dry and hot extremes in India. *Iscience*, **25**, 11. https://doi.org/10.1016/j.isci.2022.105377.

Rawat, N., Purohit, S., Negi, G.S. and Pant, D., 2017, "Perception of local people towards blazing mountain due to forest fire in changing climatic scenario of Uttarakhand Himalaya: A need for scientific intervention for sensitization and conservation and livelihood sustainability of region", Indian For., **143**, 28–32.

Raymond, C., Horton, R.M., Zscheischler, J., Martius, O., AghaKouchak, A., Balch, J., Bowen, S.G., Camargo, S.J., Hess, J., Kornhuber, K. and Oppenheimer, M., 2020, "Understanding and managing connected extreme events", *Nat. Clim. Change*, **10**, 7, 611–621. https://doi.org/10.1038/s41558-020-0790-4.

Sagar, N., Suresh, K.P., Naveesh, Y.B., Archana, C.A., Hemadri, D., Patil, S.S., Archana, V.P., Raaga, R., Nandan, A.S. and Chethan, A.J., 2024, "Forest fire dynamics in India (2005–2022): Unveiling climatic impacts, spatial patterns, and interface with anthrax incidence", *Ecol. Indic.*, **166**, 112454. https://doi.org/10.1007/s11600-023-01094-5.

Sahu, R.K., Hari, M. and Tyagi, B., 2022. "Forest fire induced air pollution over Eastern India during March 2021", *Aerosol Air Qual. Res.*, **22,** 8, 220084. https://doi.org/10.4209/aaqr.220084.

Sharma, A., Sharma, D., Panda, S.K., Sunder, M.S.S. and Kumar Dubey, S., 2024, "Seasonal analysis of long-term (1970–2020) rainfall variability using clustering and wavelet transform approach in the Mahi River Basin, India", *Acta Geophys.*, **72**, 3, 1879–1894.

Shi, M., McDowell, N., Huang, H., Zahura, F., Li, L. and Chen, X., 2025. Ecosystem leaf area, gross primary production, and evapotranspiration responses to wildfire in the Columbia River basin. *Biogeosciences*, **22**, 9, 2225-2238. https://doi.org/10.5194/bg-22-2225-2025.

Singh, D., Sharma, P., Kumar, U., Daverey, A. and Arunachalam, K., 2021. "Effect of forest fire on soil microbial biomass and enzymatic activity in oak and pine forests of Uttarakhand Himalaya, India". Ecol. Process., **10**, 1, 29. https://doi.org/10.1186/s13717-021-00293-6.

Singh, R.D., Gumber, S., Sundriyal, R.C., Ram, J. and Singh, S.P., 2024, "Chir pine forest and pre-monsoon drought determine spatial, and temporal patterns of forest fires in Uttarakhand Himalaya", *Trop. Ecol.*, **65**, 1, 32-42. https://doi.org/10.1007/s42965-023-00306-9.

Stephens, E.Z. and Homyak, P.M., 2023, "Post-fire soil emissions of nitric oxide (NO) and nitrous oxide (N_2O) across global ecosystems: a review", *Biogeochemistry*, **165**, 3, 291–309. https://doi.org/10.1007/s10533-023-01072-5.

Sun, Q., Miao, C., Hanel, M., Borthwick, A.G., Duan, Q., Ji, D. and Li, H., 2019, "Global heat stress on health, wildfires, and agricultural crops under different levels of climate warming", *Environ. Int.*, **128**, 125–136. https://doi.org/10.1016/j.envint.2019.04.025.

Sunder, M.S., Tikkiwal, V.A., Kumar, A. and Tyagi, B., 2023, "Unveiling the transparency of prediction models for spatial $PM_{2.5}$ over Singapore: comparison of different machine learning approaches with explainable artificial intelligence", *AI*, **4**, 4, 787–811. https://doi.org/10.3390/ai4040040.

Tepley, A.J., Thomann, E., Veblen, T.T., 2018, "Influences of fire–vegetation feedbacks and post-fire recovery rates on forest landscape vulnerability to altered fire regimes", *J. Ecol.*, **106**, 1925-1940. https://doi.org/10.1111/1365-2745.12950.

Thom, D., 2023, "Natural disturbances as drivers of tipping points in forest ecosystems under climate change–implications for adaptive management", *Forestry*, **96**, 3, 305-315. https://doi.org/10.1093/forestry/cpad011.

Tithi, A.C., Sohel, M.S.I., Jakariya, M. and Rana, P., 2024, "Analyzing ecosystem functions in Bangladesh's forests: a historical MODIS study", Geol. Ecol. Landsc., (ahead of print), 1–13. https://doi.org/10.1080/24749508.2024.2334516.

Wu, Z., Zheng, J., Wang, Y., Shang, D., Du, Z., Zhang, Y. and Hu, M., 2017, "Chemical and physical properties of biomass burning aerosols and their CCN activity: A case study in Beijing, China", *Sci. Total Environ.*, **579**, 1260–1268. https://doi.org/10.1016/j.scitotenv.2016.11.112.

WWF International, 2020, "Fires, Forests, and the Future: A Crisis Raging Out of Control?", WWF Report, https://wwfeu.awsassets.panda.org/downloads/wwf_fires_forests_and_the_future_report.pdf (Accessed: 1 January 2025).

Xu, W., Elberling, B. and Ambus, P.L., 2022, "Pyrogenic organic matter as a nitrogen source to microbes and plants following fire in an Arctic heath tundra", *Soil Biol. Biochem.*, **170**, 108699. https://doi.org/10.1016/j.soilbio.2022.108699.

Zhou, S., Yu, B., Huang, Y. and Wang, G., 2014, "The effect of vapor pressure deficit on water use efficiency at the subdaily time scale", *Geophys. Res. Lett.*, **41**, 14, 5005–5013. doi.org/10.1002/2014GL060741.

Appendix

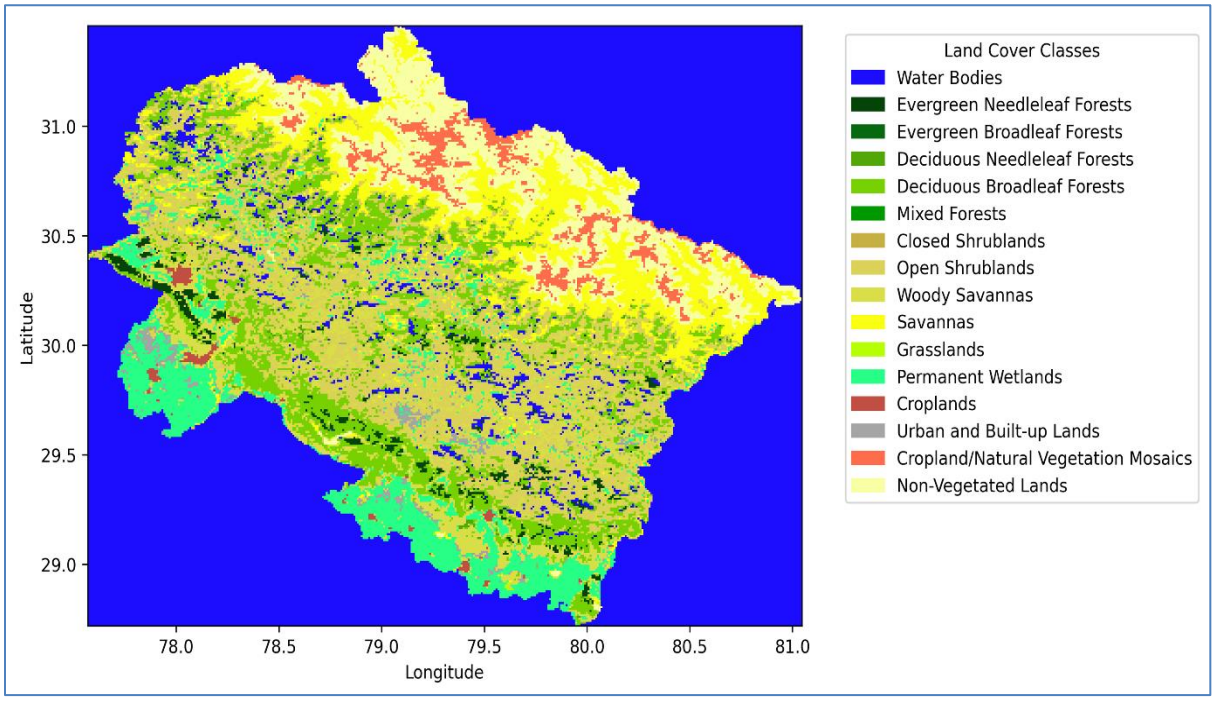

Fig. S1. Land Use/Land cover for Uttarakhand using MODIS data

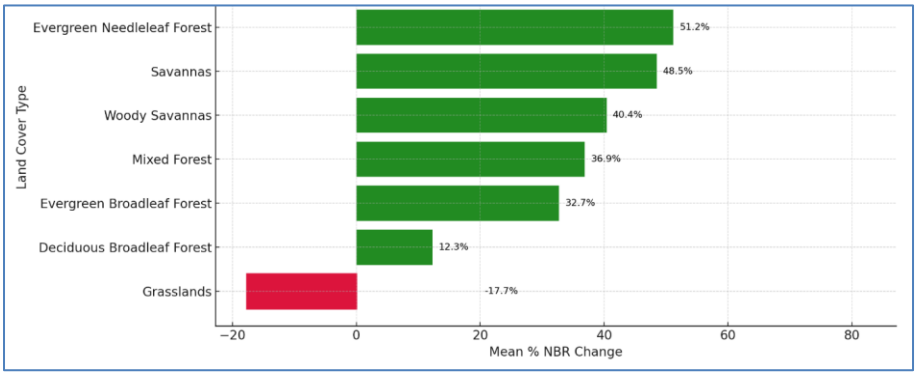

Fig. S2. NBR pre and post fire percentage change over LULC classes

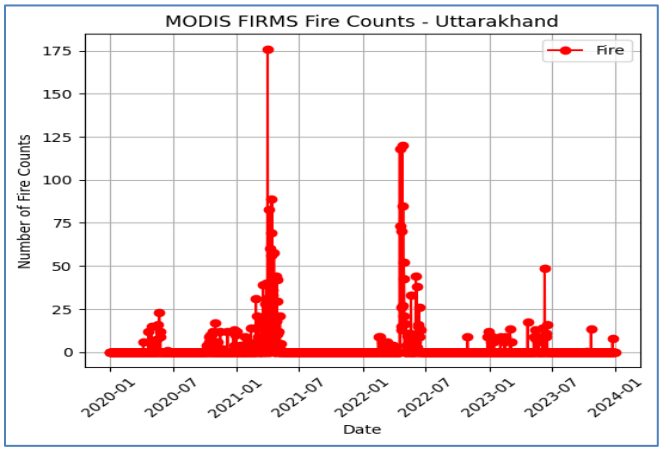

Fig. S3. Fire counts from 2020 to 2023 using FIRMS dataset

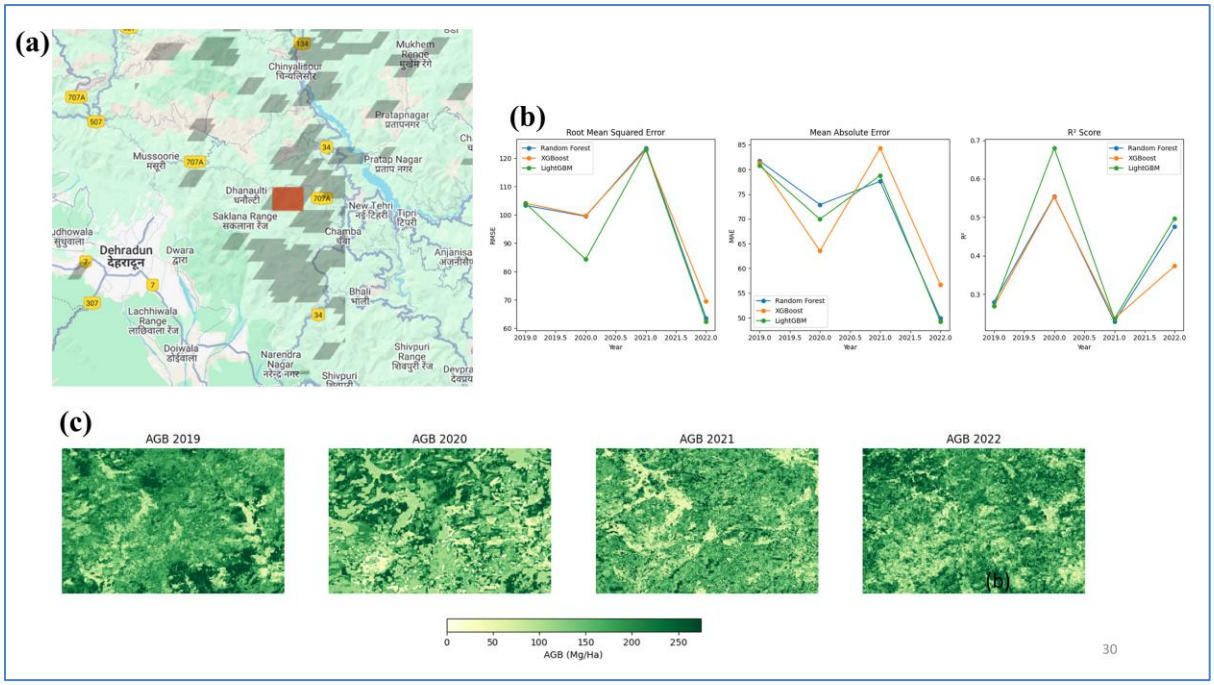

Figs. S4(a-c). Spatial variation of Biomass estimation and error metrics (a) Shows the location of the fire patch highlighted in brown box and grey are fire locations (b) show the accuracy error with different ML models RMSE, MAE and R^2 (c) Spatial representation of Predicted AGB (Mg/ha)

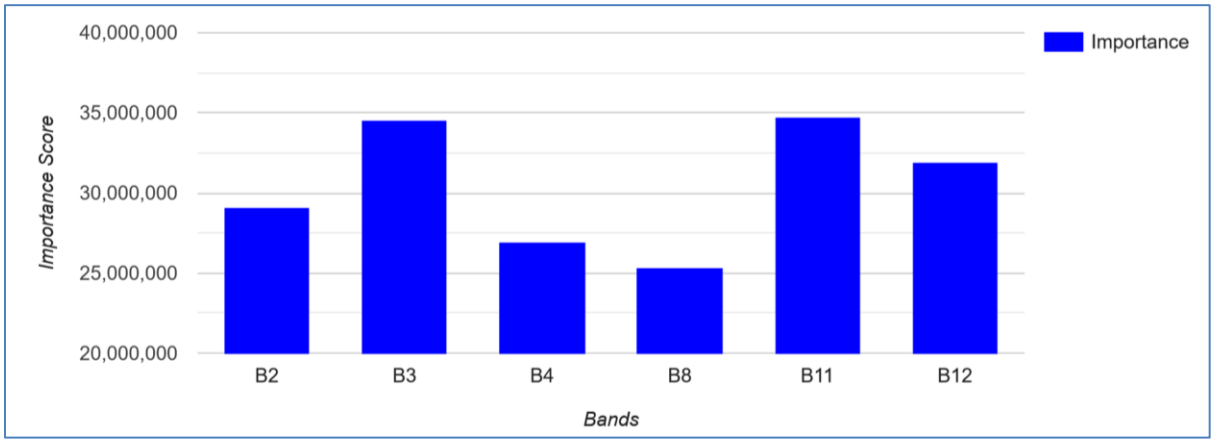

Fig. S5. Feature importance of the Random forest model for predicted AGB (Mg/ha)